Available online at www.sciencedirect.com
SCIENCE DIRECT®
Chemical Physics 307 (2004) 91–95
Chemical Physics
www.elsevier.com/locate/chemphys

Charge transfer states of C_2 in Kr clusters

S. Fiedler, H. Kunttu, J. Eloranta *

Department of Chemistry, University of Jyväskylä, P.O. Box 35, Survontie 9, Jyväskylä 40500, FIN-40014, Finland

Received 5 February 2004; accepted 7 April 2004
Available online 11 September 2004

Abstract

Ab initio and diatomics-in-ionic-systems (DIIS) calculations are carried out for the C_2–Kr pair and C_2–Kr_n clusters, respectively. Energetics and transition dipole moments between the ground and excited states are obtained from the calculations. This data is then used to predict the UV charge transfer absorption spectrum of C_2 embedded in Kr_n clusters with $n = 1$, 12, and 224. The results reveal discrete structure in the computed UV spectrum, which is mainly related to the spin–orbit splitting of Kr^+.

1. Introduction

Atomic and molecular charge transfer states in doped rare gas solids, such as Ar, Kr, and Xe, have been studied extensively by both experimental and theoretical methods. In most cases UV absorption or fluorescence experiments were carried out using atomic dopants that have relatively high electron affinities, such as halogens [1–3], hydrogen atoms [4–6], sulfur atoms [7], or oxygen atoms [8]. In most cases the high-energy side of the charge transfer absorptions is accompanied with an additional discrete set of lines, which have been attributed to delocalization of charge within the solid [1–3,6]. It has been further observed in the experiments that excitation of these transitions may lead to permanent charge separation in the solid [3]. Energetically both absorption and emission origins are clearly shifted as compared to the gas phase, indicating strong interaction between the dopant and the rare gas solid.

Diatomic radicals, such as ·OH and ·CN, have also been shown to posses charge transfer states when trapped within rare gas solids [9,10]. The UV absorption spectra display nearly identical features as compared to the rare gas solids with atomic dopants. The major difference arises, however, from the fact that the diatomic constituent has additional internal degrees of freedom, which usually provide effective non-radiative relaxation channels. In practice, fluorescence has only been observed from the internal electronic states of the diatomic molecule rather than the charge transfer state itself [10].

Theoretical descriptions of the charge transfer states have usually been based on diatomics-in-ionic-systems (DIIS) or very limited ab initio methods [10,11]. Due to computational cost of typical multi configuration self-consistent field (MCSCF) or multi-reference configuration interaction (MRCI) calculations, they are limited to describe few atom systems only. The DIIS method, which is an extension of the diatomics-in-molecules (DIM) formalism, has better computational scalability and has also been shown to produce highly accurate results [12]. The first application of DIIS to model the charge transfer states in rare gas atom clusters was given by Last and George [13]. Since then it has also been applied in theoretical description of the charge transfer absorptions of diatomic species in rare gas solids [10].

In this paper we have studied the ground and charge transfer states between C_2 and Kr_n rare gas clusters. First we performed MCSCF calculations of C_2–Kr pair potentials and transition dipole moments. Then the

* Corresponding author. Fax: +358 14 2602551.
E-mail address: eloranta@cc.jyu.fi (J. Eloranta).

0301-0104/$ - see front matter © 2004 Elsevier B.V. All rights reserved.
doi:10.1016/j.chemphys.2004.04.031

DIIS method was used to calculate the energetics of the extended C_2–Kr_n system. Finally, we will provide theoretical prediction of the charge transfer absorption spectrum of C_2 in Kr clusters. The largest calculated cluster ($n = 224$), which corresponds to 11 solvation shells, will be taken to resemble a solid Kr matrix.

2. Method

The neutral and ionic C_2–Kr ground state pair potentials were computed in both linear and broadside (C_{2v}; "T-shape") geometries by the spin restricted coupled cluster method with single, double, and perturbative triple excitations (CCSD(T)) [14,15] with Dunning's correlation consistent basis cc-vqz (VQZ) for carbon [16] and the Stuttgart group effective core potential (ECP) basis for krypton [17]. This combination of atomic basis we will denote as VQZ*. For all CCSD(T) calculations we further augmented the VQZ basis (e.g., aug-cc-vqz), denoted by AVQZ*. Basis set superposition error correction using the method of Boys and Bernardi [18] was carried out for all CCSD(T) calculations. All the CCSD(T) calculations fulfilled the standard single excitation amplitude test [19]. Since the traditional CCSD(T) method is only applicable to the lowest state of given symmetry, the excited states cannot be obtained with this approach. We have used the MCSCF with complete active space (CAS) to compute the excited states [20,21]. The active space was taken to include the outmost p-orbital frame of Kr as well as the four lowest occupied and four unoccupied molecular orbitals of C_2. This calculation can describe the static electron correlation properly but not the dynamic correlation. The latter energy contribution could be included in the calculation by carrying out a CI calculation (e.g., MRCI) using the MCSCF result as reference. This approach was used in our previous study on the CN–Kr system [10]. However for C_2–Kr system it failed due to very high density of states, curve crossings, and appearance of dense manifold of Rydberg states. Thus we were forced to abandon the CI calculation stage and neglect the dynamic correlation contribution. Finally, the Kr–Kr pair interaction was taken from semi-empirical model of Aziz [22]. All the ab initio calculations were carried out using the MOLPRO 2002.6 suite of programs [23].

The present DIIS calculations closely follow those presented in [10], where exact formulation of the DIIS Hamiltonian and related expressions are given. Firstly, we consider the freely rotating C_2 molecule as "atomic entity" that behaves like an atom having one electron hole in its p-orbital frame. This approximation avoids treatment of the intramolecular dynamics of C_2, which in effect declares the vibrational and rotational coupling of the dopant to the lattice as negligible. The Hamiltonian is essentially constructed from the pair potential data by carrying out rotations between the diatomic and the laboratory frames. The suitable pair potential data is provided by the ab initio calculations as described above. Finally, the effective spin–orbit interaction contribution is added to the Hamiltonian using the atoms-in-molecules approach [24]. The zero-overlap DIM assumption, which has its typical problems in connecting the ground and ionic states properly, is not a concern as the energy gap between the ground and ionic states is large. Consequently we ignore completely the mixing between the states. The pair potentials were broken into exchange and Coulomb parts. The exchange part is pair-wise additive when rotated to proper frame and as such it is used directly in constructing the DIIS Hamiltonian. However, the Coulomb part is not properly pair-wise additive and therefore it is replaced by explicit evaluation of the electric field from the point charges with dielectric screening. Given a static configuration of the C_2–Kr_n system, a DIIS calculation will yield the ground and excited state energies as well as their associated eigenvectors. The eigenvectors can be used in computing the transition moment between the states by using the diatomic transition moment data from ab initio calculations as input. The transition dipole input is necessary, as we have ignored mixing in our DIIS construct. All the calculations are subject to natural boundaries.

The UV absorption spectrum was calculated by first obtaining the ground state minimum energy configuration at 0 K with the simulated annealing method and then carrying out a single point calculation to obtain transition energies and transition moments. The resulting stick spectrum was convoluted with a Lorentzian function in order to account for electronic dephasing and other broadening mechanisms that are not present in the current theoretical model. For a small cluster ($n = 12$) we used a direct classical Monte-Carlo sampling with $T = 20$ K to approximately model the zero-point distribution of the system.

3. Results and discussion

By considering the known energetics and harmonic frequencies of the $C_2X\,^1\Sigma_g$ and a $^3\Pi_u$ states, thermal population of the a $^3\Pi_u$ state would be negligible at temperatures of typical experiments. The energy difference between the lowest vibrational states is ca. 130 meV whereas kT is ~2.5 meV at 30 K [25]. Thus, it is sufficient to consider only the ground state C_2 in the following DIIS calculations. The pair interaction between C_2(X) and Kr as obtained from the CCSD(T) calculations are shown in Fig. 1 for both linear and broadside approaches. The previously published C_2(X)–Ar potentials by using a similar computational approach are also shown for Patel et al. [26]. For both Ar and Kr the linear

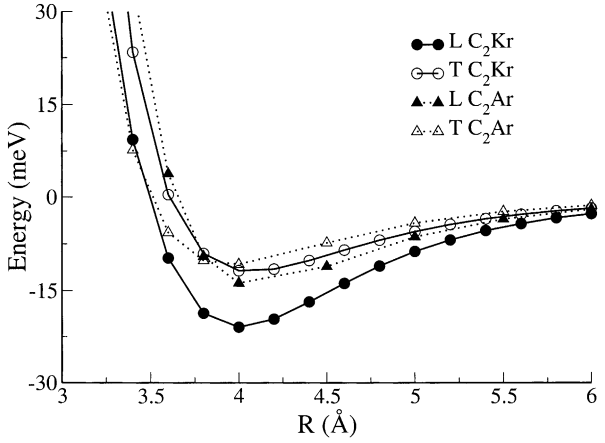

Fig. 1. Calculated pair potentials from CCSD(T)/AVQZ* calculations are shown for C_2–Kr and C_2^-–Kr. The previously published C_2–Ar pair potential is shown for reference [26]. "L" and "T" refer to the direction of approach for the rare gas atom, e.g., linear or broadside.

geometry is favored over the broadside approach. An expected overall trend is that the C_2–Kr potentials are more bound than the C_2–Ar potentials due to larger polarizability of the Kr atom. The $C_2^-(X)$–Kr pair potential was also obtained by the CCSD(T) method and the resulting data was fitted to the following analytic form:

$$V(r) = a e^{-(r-r_o)^{2/\alpha}} - \frac{c_4}{r^4} - \frac{c_6}{r^6}, \quad (1)$$

where least-squares fit yielded $a = 19.55$ eV, $r_o = 0.910$ Å, $\alpha = 1.629$ Å^2, $c_4 = 17.76$ eV Å^4, and $c_6 = 146.67$ eV Å^6. In principle the accuracy of both CCSD(T) and MCSCF calculations could be enhanced by increasing size of the applied basis set. However, both C_2 and Kr basis sets should be improved simultaneously in a balanced manner. At present improved valence part for the Kr ECP basis is not available. In previous studies, combining AVQZ and the Stuttgart ECP basis with its standard valence basis functions has given good results [10,11]. As the CCSD(T) method allows accurate counterpoise correction, the ground state potentials are expected to be more accurate than the corresponding MCSCF potentials. Overall, the linear and broadside C_2–Kr potentials were very similar to the CN–Kr system and as such C_2 molecule should behave as a free rotor in Kr_n clusters [10]. Experimental verification free molecular rotation appears not to be available in the literature. Furthermore, inspection of linear and broadside pair potentials yield nearly identical equilibrium bond lengths and binding energies.

For charge transfer states, only MCSCF calculation can be carried out and thus it has two obvious sources of error: basis set superposition error and lack of dynamic electron correlation. The latter contribution can be estimated from our previous CN–Kr calculations, where energies of the ionic states were lowered by ~100 meV around the potential minimum of the ground state [10]. Results from the MCSCF/VQZ* calculations are shown in Fig. 2. All the charge transfer state potentials show the characteristic $\sim -1/r$ Coulombic tail at large nuclear separation. The calculated potential energy curves predict an electronic absorption between the ground and the lowest ionic state of C_2–Kr at 6.98 eV (~172 nm) and the relaxed fluorescence at 6.78 eV (~182 nm). The MCSCF calculations also provide the transition dipole moments between ground and charge transfer states as shown in Fig. 3. It can be clearly seen that only the linear $^1\Sigma$ state has considerable transition dipole moment, whereas all other states can mostly be neglected. At 4 Å the transition dipole moment is ~4 Debye, which should make the transition slightly more intense than observed for the CN–Kr system [10].

Next, we consider energetics of C_2–Kr_n clusters by using the DIIS construct. Based on the simulated annealing optimization with the DIIS method, the ground state C_2 molecule occupies a singly substitutional site in an extended Kr cluster. The lattice shows mostly face-centered-cubic (FCC) structure in the vicinity of C_2. The calculated UV absorption spectra for the C_2–Kr_n clusters ($n = 12$ and $n = 224$) are shown in Fig. 4. As demonstrated in Fig. 3 only the linear geometry has significant transition dipole between the ground and charge transfer state and therefore makes the linear geometry dominant in calculating the energetics for the UV absorption spectrum. Consequently, the DIIS calculation of the spectrum is not very sensitive to the broadside charge transfer pair potential. In the case of $n = 12$, which consists of one shell of Kr atoms around C_2, four distinct absorptions were observed. The spectrum shows the approximate $J = 1/2$ and $J = 3/2$ bands, which were identified earlier [10]. Thus, the spin–orbit splitting of Kr^+ can be obtained from the energy difference between these bands. Furthermore, the bands have been further

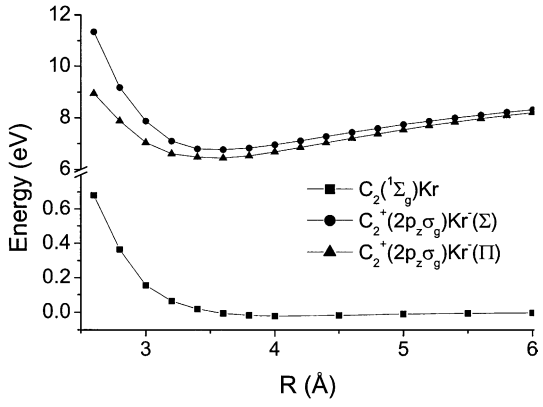

Fig. 2. Calculated pair potentials from MCSCF/VQZ* calculations are shown for the ground and charge transfer states of linear C_2–Kr. Note that the broadside approach yields essentially identical potentials.

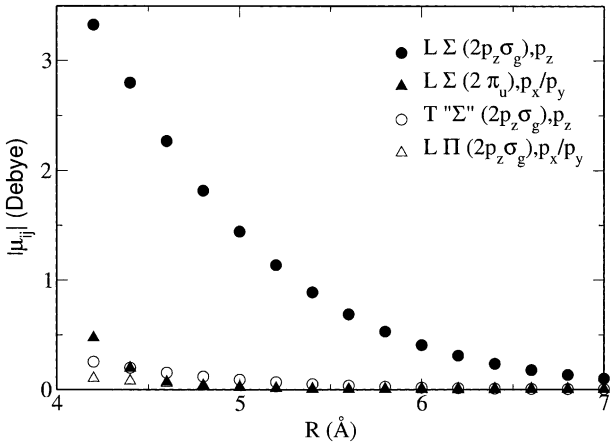

Fig. 3. Transition dipole moments connecting the ground and charge transfer states are shown. The results were obtained from MCSCF/VQZ* calculations. "L" and "T" refer to the direction of approach for the rare gas atom, e.g., linear or broadside.

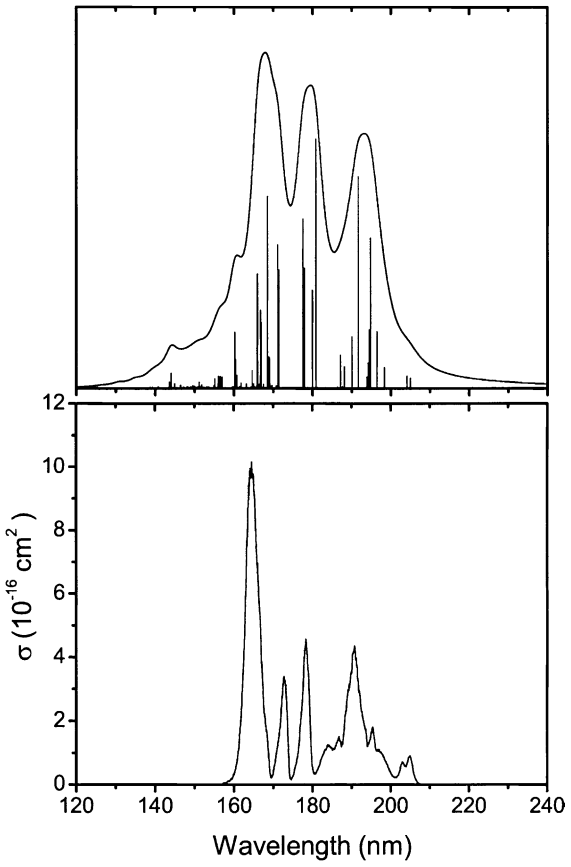

Fig. 4. The calculated UV absorption spectra of C_2 embedded in Kr_n clusters with $n = 224$ (upper panel) and $n = 12$ (lower panel) are shown.

split into additional components, which could not be classified due to high number of contributing states. In order to predict the UV absorption spectrum in extended solid, a large cluster with $n = 224$ was calculated. In this case the UV absorption spectrum displays three main features located at 190, 175, and 165 nm. The splitting between 190 and 170 nm coincides with the spin–orbit splitting of Kr^+ ion ($\xi \sim 0.7$ eV). Again the $J = 1/2$ component is split and it is not possible to label this state properly. Overall, the calculations show that the main contribution to the energetics in the absorption spectrum comes from the first solvent shell (see Fig. 4). Since dynamic electron correlation was not included in the pair potential calculations, we expect that all the three spectral features will be slightly red shifted with respect to calculated values. Direct fluorescence from the charge transfer state may not be observable due to non-radiative transitions that lead to population of internal excited states of C_2. Similar fluorescence quenching scheme has been observed for the CN radical in Kr matrix [10]. Thus in order to experimentally identify the charge transfer states of C_2 in solid Kr, the UV absorption spectrum should be recorded in the wavelength region shown in Fig. 4.

References

[1] M.E. Fajardo, V.A. Apkarian, J. Chem. Phys. 85 (1986) 5660.
[2] M.E. Fajardo, V.A. Apkarian, J. Chem. Phys. 89 (1988) 4102.
[3] M.E. Fajardo, V.A. Apkarian, J. Chem. Phys. 89 (1988) 4124.
[4] F. Wittl, M.J. Creuzburg, J. Mol. Struct. 222 (1990) 127.
[5] F. Wittl, J. Eberlein, T. Epple, M. Dechant, M.J. Creuzburg, J. Chem. Phys. 98 (1993) 9554.
[6] H. Kunz, J.G. McCaffrey, M. Chergui, R. Schriever, Ö. Ünal, N. Schwentner, J. Chem. Phys. 95 (1991) 1466.
[7] S. Tanaka, H. Kajihara, S. Koda, V.A. Apkarian, Chem. Phys. Lett. 233 (1995) 555.
[8] M.S. Gudipati, M. Kalb, Chem. Phys. Lett. 307 (1999) 27.
[9] H. Kunz, H.G. NcCaffrey, M. Chergui, R. Schriever, Ö. Ünal, N. Schwentner, J. Luminesc. 48–49 (1991) 621.
[10] S.L. Fiedler, K. Vaskonen, J. Ahokas, H. Kunttu, J. Eloranta, V.A. Apkarian, J. Chem. Phys. 117 (2002) 8867.
[11] J. Eloranta, H. Kunttu, J. Chem. Phys. 113 (2000) 7446.
[12] B.L. Grigorenko, A.V. Nemukhin, V.A. Apkarian, J. Chem. Phys. 108 (1998) 4413.
[13] I. Last, T.F. George, J. Chem. Phys. 87 (1987) 1183.
[14] P.J. Knowles, C. Hampel, H.-J. Werner, J. Chem. Phys. 99 (1993) 5219.
[15] J.D. Watts, J. Gauss, R.J. Bartlett, J. Chem. Phys. 98 (1993) 8718.
[16] R.A. Kendall, T.H. Dunning Jr., R.J. Harrison, J. Chem. Phys. 96 (1992) 6796.
[17] A. Nicklass, M. Dolg, H. Stoll, H. Preuss, J. Chem. Phys. 102 (1995) 8942.
[18] F. Boys, F. Bernardi, Mol. Phys. 19 (1970) 553.
[19] T.J. Lee, P.R. Taylor, Int. J. Quantum Chem. 23 (1989) 4936.
[20] H.-J. Werner, P.J. Knowles, J. Chem. Phys. 82 (1985) 5053.
[21] P.J. Knowles, H.-J. Werner, Chem. Phys. Lett. 115 (1985) 259.
[22] R.A. Aziz, M.J. Slaman, Mol. Phys. 58 (1986) 697.
[23] H.-J. Werner, P.J. Knowles, R.D. Amos, A. Bernhardsson, A. Bering, P. Celani, D.L. Cooper, M.J.O. Deegan, A.J. Dobbyn, F. Eckert, C. Hampel, G. Hetzer, P.J. Knowles, T. Korona, R. Lindh, A.W. Lloyd, S.J. McNicholas, F.R. Manby, W. Meyer, M.E. Mura, A. Niclass, P. Palmieri, R. Pitzer, G. Rauhut, M. Schütz, U. Schumann, H. Stoll, A.J. Stone, R. Tarroni, T.

Thorsteinsson, H.-J. Werner, MOLPRO 2002.6 package designed by H.-J. Werner, P.J. Knowles.
[24] F. Mies, Phys. Rev. A 7 (1973) 942.
[25] M. Martin, J. Photochem. Photobiol. A 66 (1992) 263.
[26] K. Patel, P.R. Butler, A.M. Ellis, M.D. Wheeler, J. Chem. Phys. 119 (2003) 909.